

Hydroxamic Acids as Potent Inhibitors of Fe^{II} and Mn^{II} *E. coli* Methionine Aminopeptidase: Biological Activities and X-ray Structures of Oxazole Hydroxamate–*EcMetAP*–Mn Complexes

Florian Huguet,^[a] Armelle Melet,^[a] Rodolphe Alves de Sousa,^[a] Aurélie Lieutaud,^[b] Jacqueline Chevalier,^[b] Laure Maigre,^[b] Patrick Deschamps,^[c] Alain Tomas,^[c] Nicolas Leulliot,^[c] Jean-Marie Pages,^[b] and Isabelle Artaud^{*,[a]}

New series of acids and hydroxamic acids linked to five-membered heterocycles including furan, oxazole, 1,2,4- or 1,3,4-oxadiazole, and imidazole were synthesized and tested as inhibitors against the Fe^{II}, Co^{II}, and Mn^{II} forms of *E. coli* methionine aminopeptidase (MetAP) and as antibacterial agents against wild-type and *acrAB* *E. coli* strains. 2-Aryloxazol-4-ylcarboxylic acids appeared as potent and selective inhibitors of the Co^{II} MetAP form, with IC₅₀ values in the micromolar range, whereas 5-aryloxazol-2-ylcarboxylic acid regioisomers and 5-aryl-1,2,4-oxadiazol-3-ylcarboxylic acids were shown to be inefficient against all forms of *EcMetAP*. Regardless of the heterocycle, all the hydroxamic acids are highly potent inhibitors and are selective for the Mn^{II} and Fe^{II} forms, with IC₅₀ values between 1 and 2 μM. One indole hydroxamic acid that we previously reported as a potent inhibitor of *E. coli* peptide deformylase also demonstrated efficiency against *EcMetAP*. To gain insight into

the positioning of the oxazole heterocycle with reversed substitutions at positions 2 and 5, X-ray crystal structures of *EcMetAP*–Mn complexed with two such oxazole hydroxamic acids were solved. Irrespective of the [metal]/[apo-MetAP] ratio, the active site consistently contains a dinuclear manganese center, with the hydroxamate as bridging ligand. Asp97, which adopts a bidentate binding mode to the Mn2 site in the holoenzyme, is twisted in both structures toward the hydroxamate bridging ligand to favor the formation of a strong hydrogen bond. Most of the compounds show weak antibacterial activity against a wild-type *E. coli* strain. However, increased antibacterial activity was observed mainly for compounds with a 2-substituted phenyl group in the presence of the nonapeptide polymyxin B and phenylalanine–arginine–β-naphthylamide as permeabilizer and efflux pump blocker, respectively, which boost the intracellular uptake of the inhibitors.

Introduction

The spread and dissemination of multidrug-resistant bacteria is a major limitation to the treatment of infectious diseases with known antibiotics. One strategy for combating this is to focus on new targets involved in biochemical processes that are essential to bacterial growth, such as N-terminal methionine excision (NME).^[1] In prokaryotes all nascent polypeptide chains are initiated with an *N*-formylmethionine residue, and NME requires the action of peptide deformylase (PDF) and methionine aminopeptidase (MetAP) to successively cleave the formyl group and the N-terminal methionine. Deletion of the gene that codes for MetAP was found to be lethal for *Escherichia coli*^[2] and *Salmonella typhimurium*.^[3] Therefore, MetAP has been selected as a target of interest in the search for new antibacterial agents. MetAPs belong to the large family of metalloproteases^[4] and have been extensively characterized over the last decade. However, unlike most enzymes of this family, the nature of the metal cation at the active site in vivo as well as the nuclearity of the metal center are still a subject of controversy. These metalloproteases are activated by several divalent metal cations such as Co^{II}, Mn^{II}, Ni^{II}, Zn^{II} or Fe^{II}. The enzymatic activity of *E. coli* MetAP (*EcMetAP*) is maximal in the presence of only 1 equivalent of Co^{II},^[5] Fe^{II},^[5] or Mn^{II},^[6] suggesting that

MetAP is a mononuclear metalloprotease. However, MetAP can bind two metal cations, yet the binding affinities for the first and second metal cations differ by three orders of magnitude; for example *EcMetAP* loaded with Co^{II} shows $K_{d1} = 300 \pm 50$ nM and $K_{d2} = 2.5 \pm 0.5$ mM.^[5] The high-affinity binding site was assigned to the histidine-containing site on the basis of EXAFS experiments with the iron,^[7] cobalt,^[7] and manganese forms,^[6] a hypothesis that has been confirmed by recent X-ray crystal structures of monometallated Mn^{II} forms of *EcMetAP* com-

[a] Dr. F. Huguet,⁺ Dr. A. Melet,⁺ Dr. R. Alves de Sousa, Dr. I. Artaud
Laboratoire de Chimie et Biochimie Pharmacologiques et Toxicologiques
UMR 8601, CNRS Université Paris Descartes
45 rue des Sts. Pères, 75270 Paris Cedex 06 (France)
E-mail: isabelle.artaud@parisdescartes.fr

[b] Dr. A. Lieutaud, Dr. J. Chevalier, Dr. L. Maigre, Dr. J.-M. Pages
UMR-MD1, Transporteurs Membranaires Aix-Marseille Université
IRBA, Marseille (France)

[c] Dr. P. Deschamps, Prof. A. Tomas, N. Leulliot
UMR 8015, CNRS Université Paris Descartes
Laboratoire de Cristallographie et RMN Biologiques, Paris (France)

[*] These authors contributed equally to this work.

Supporting information for this article is available on the WWW under <http://dx.doi.org/10.1002/cmdc.201200076>.

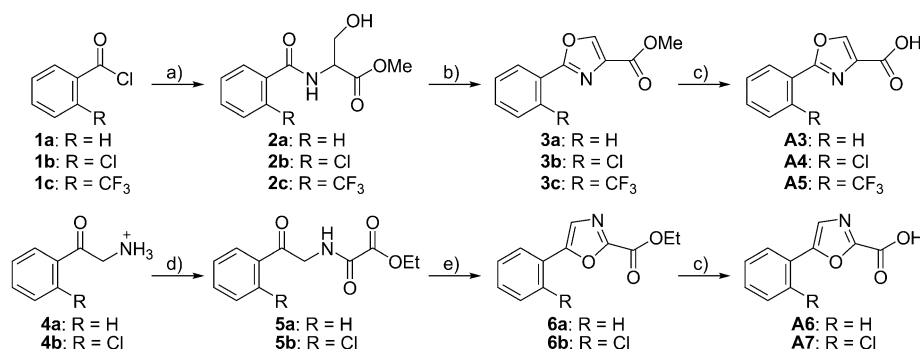
plexed with norleucine phosphonate^[8] and a hydrazide inhibitor.^[9] In addition to these results that support a mononuclear form of MetAP, MCD and atomic absorption spectrometry data^[10] as well as EPR experiments^[11,12] have led to the assumption that even at low metal content, a small fraction of the active site is dinuclear due to a weak cooperative binding of metal cations. Regarding the identity of the metal cation in vivo, *EcMetAP* is suggested to be an iron enzyme on the basis of whole-cell metal analyses combined with activity measurements.^[13–15] The trend is now to find metal-specific inhibitors^[16,17] that can bind a mononuclear or dinuclear form of MetAP. In this prospect, the hydroxamic acid moiety is a versatile functional group that can serve as a bidentate ligand to chelate metal ions at mono- or dinuclear enzyme active sites. Accordingly, hydroxamates are promiscuous inhibitors of most metalloenzymes containing divalent cations including Zn^{II}, Mn^{II}, Ni^{II}, or Fe^{II}. By far the most common mode of metal binding is through the deprotonated hydroxamate and carbonyl oxygen atom, which can adopt an (O,O) or (O, μ O) chelating mode, depending if the active site binds one or two metal ions. Hydroxamic acids are strong inhibitors of metalloproteases,^[18] whether mononuclear as with matrix metalloproteases^[19] and peptide deformylases,^[20] or dinuclear, as with aminopeptidases^[21] and ureases.^[22]

In continuation of our ongoing research on new antibacterial agents that target the NME process in bacteria, we have extended our work from PDF inhibitors^[23,24] to MetAP inhibitors. We previously prepared several indole hydroxamic acids as potent PDF inhibitors,^[23,24] and herein we describe the synthesis of a new series of such derivatives linked to five-membered heterocycles including furan, oxazole, oxadiazole, and imidazole to favor interactions with the protein backbone of MetAP. Their inhibitory potencies, as well as those of some of the indole derivatives, were evaluated against Co^{II}, Mn^{II}, and Fe^{II} forms of *EcMetAP*; we then assessed their antibacterial activities against Gram-positive and Gram-negative bacteria. These data were compared with those of the corresponding acids, for compounds that were sufficiently stable for isolation. In the furan series, 5-arylfuranyl-2-carboxylic acids and 5-(2-chlorophenyl)furanylhydroxamic acid were previously prepared and tested by Ye et al.^[16,17] Two X-ray crystal structures of the Mn^{II} form with oxazole hydroxamic acids were solved, highlighting a specific interaction of the hydroxamic moiety with a dinuclear active site, even at low metal content.

Results and Discussion

Chemistry

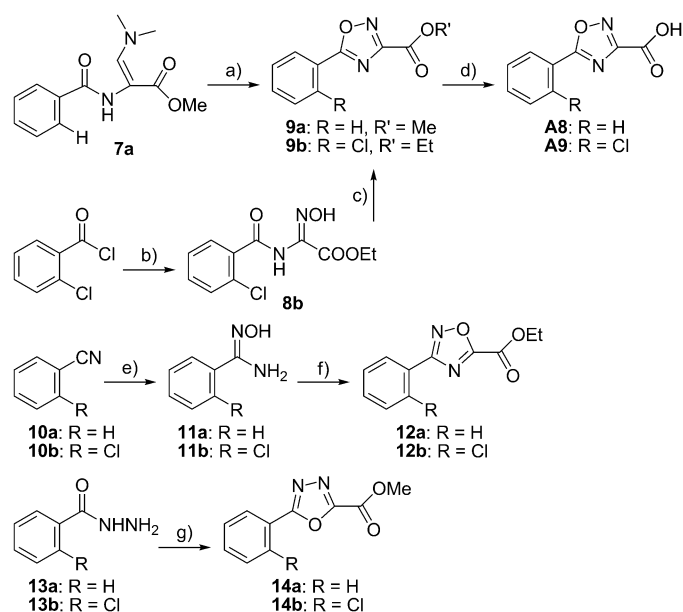
Two regioisomers of oxazole derivatives were prepared in which the oxazole ring was substituted by an aryl group and a carboxylic acid methyl ester at positions 2 and 5, or 5 and 2, as outlined in Scheme 1. 2-Aryloxazol-4-ylcarboxylic acid



Scheme 1. Synthesis of oxazole acids. *Reagents and conditions:* a) $\text{NH}_2\text{CH}(\text{CH}_2\text{OH})\text{COOMe}\cdot\text{HCl}$, Et_3N , CH_2Cl_2 , RT, 36 h; b) 1. Deoxo-Fluor, CH_2Cl_2 , 2. BrCCl_3 , DBU, 0°C , 4 h; c) 1. LiOH , $\text{H}_2\text{O}/\text{THF}$, 2. HCl , RT, 1 h; d) ClCOCOOEt , Et_3N , CH_2Cl_2 , RT, 72 h; e) POCl_3 , reflux, 3.5 h.

methyl esters (**3a**, **3b**, and **3c**) were obtained by dehydrative cyclization of the corresponding β -hydroxyamides (**2a**, **2b**, and **2c**) with bis(2-methoxyethyl)aminosulfur trifluoride (Deoxo-Fluor) at -10°C , followed by in situ oxidation of the adduct at 0°C with bromotrichloromethane and 1,8-deazabicyclo[5.4.0]undec-7-ene (DBU).^[25] The corresponding 5-phenyloxadiazol-2-yl- and 5-(2-chlorophenyl)oxadiazol-2-ylcarboxylic acid ethyl esters **6a** and **6b**, respectively, were synthesized by cyclization, in phosphoryl chloride, of the *N*-(2-oxo-2-arylethyl)oxalamide acid ethyl esters **5a** and **5b** prepared by condensation of 2-aminoacetophenone **4a** or 2-amino-1-(2-chlorophenyl)ethanone **4b** with ethyl 2-chloro-2-oxoacetate.^[26] Finally, saponification of the esters **3a**, **3b**, and **3c**, and **6a** and **6b** under mild conditions with aqueous lithium hydroxide in tetrahydrofuran^[26,27] afforded the corresponding acids **A3–A7**.

Synthetic pathways of the various oxadiazole esters and acids are shown in Scheme 2. 1,2,4-Oxadiazole (two regioisomers) as well as 1,3,4-oxadiazole derivatives were synthesized. Methyl 2-phenyllamino-3-dimethylaminopropenoate **7a** was treated in aqueous hydrochloric acid with sodium nitrite at 0°C and left at room temperature to afford the 5-phenyl-1,2,4-oxadiazol-3-ylcarboxylic acid methyl ester **9a**.^[28] Under the same conditions, treatment of the 2-chlorophenyl analogue of **7a**^[28] failed to produce the corresponding oxadiazole. However, **9b** was readily obtained by condensation of ethyl-2-oxime acetate^[29,30] with 2-chlorobenzoyl chloride followed by subsequent cyclization of the adduct **8b** in *N,N*-dimethylformamide at 150°C .^[31] The 3-aryl-1,2,4-oxadiazol-5-carboxylic acid ethyl ester regioisomers were prepared in two steps. Condensation of the aryl nitriles **10a** and **10b** with hydroxylamine in a mixture of methanol and water at reflux afforded the amidoximes **11a**



Scheme 2. Synthesis of oxadiazole esters and acids. *Reagents and conditions:*

a) HNO_2 , H_2O , 0°C , 1 h; b) $\text{EtOCOC}(\text{NH}_2)\text{NOH}$, Et_3N , CH_2Cl_2 , 0°C , 1 h; c) DMF , 150°C , 4 h; d) 1. LiOH , $\text{H}_2\text{O}/\text{THF}$, 2. HCl , RT, 1 h; e) $\text{NH}_2\text{OH}\cdot\text{HCl}$, Na_2CO_3 , $\text{H}_2\text{O}/\text{MeOH}$, reflux, 12 h; f) ClCOCOOEt , $i\text{Pr}_2\text{EtN}$, THF , reflux, 2.5 h; g) 1. ClCOCOOEt , Et_3N , CH_2Cl_2 , 2. TsCl , CH_2Cl_2 , 0°C , 1 h.

and **11b**. Further reaction with ethyl 2-chloro-2-oxoacetate in tetrahydrofuran at reflux yielded the 3-aryl-1,2,4-oxadiazolyl-5-carboxylic acid ethyl esters **12a** and **12b**.^[29] 1,3-Oxadiazole derivatives **14a** and **14b** were prepared by treatment of the aryl hydrazides **13a** and **13b** with methyl 2-chloro-2-oxoacetate in dichloromethane at 0°C , followed by cyclization at room temperature of the methyl 2-(arylhydrazinyl)-2-oxoacetate intermediates with tosyl chloride.^[32] Saponification of the oxadiazole esters **9a** and **9b** with aqueous lithium hydroxide in methanol afforded the 5-aryl-1,2,4-oxadiazolyl-2-carboxylic acids **A8** and **A9**. The same treatment applied to the esters **12a**, **12b**, **14a**, and **14b**, however, did not provide the expected acids, but instead the decarboxylated aryl oxadiazoles, as previously reported.^[33]

5-(2-Chlorophenyl)-1H-imidazole-2-carboxylic acid **A14** was prepared by following a previously reported method^[34] by reaction of 3,3,3-trifluoro-2-oxopropanal with 2-chlorobenzaldehyde and ammonia in methanol, followed by saponification. Finally, 5-(2-chlorophenyl)furan-2-yl-carboxylic acid **A1** and 5-(2-trifluoromethylphenyl)furan-2-yl-carboxylic acid **A2** were prepared as previously described by Huang et al.^[17]

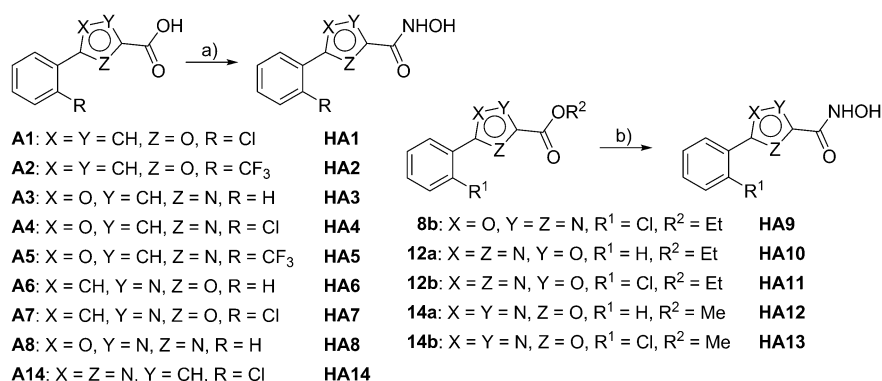
Hydroxamic acids (for a review, see Yang and Lou^[35]) were synthesized by following two routes, whether the starting

compound was the acid or the ester, as shown in Scheme 3. Carboxylic acids were activated by isobutyl chloroformate to form mixed anhydrides, which were then treated with *O*-(*tert*-butyldimethylsilyl)hydroxylamine to give the corresponding *O*-protected hydroxamic acids. Final deprotection with tetrabutylammonium fluoride in tetrahydrofuran afforded the hydroxamic acids^[24] **HA1–HA8** and **H14**. Alternatively, direct reaction of esters **8b**, **12a**, **12b**, **14a**, and **14b** with NH_2OK in methanol at room temperature^[36] resulted in the clean formation of hydroxamic derivatives **HA9–HA13**.

In vitro activity toward the Co^{II} , Mn^{II} , and Fe^{II} metalloforms of EcMetAP

The inhibitory activity of all synthesized compounds was evaluated toward EcMetAP loaded with Co^{II} , Mn^{II} , and Fe^{II} ; the resulting IC_{50} values are listed in Table 1. IC_{50} values were determined at a $[\text{metal}]/[\text{apo-MetAP}]$ ratio of 5 and a metal concentration of $15\text{ }\mu\text{M}$. Under these assay conditions, based on the very different binding constants of the two metal cations,^[5,37] only the higher-affinity metal binding site (assigned to the His-containing site) is expected to be occupied, and the active enzyme is presumably monometallated.^[7,8]

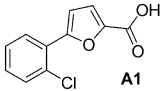
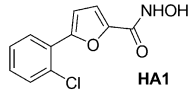
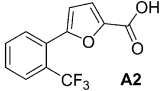
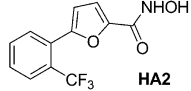
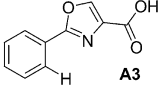
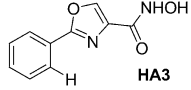
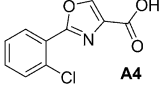
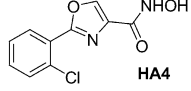
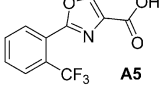
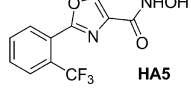
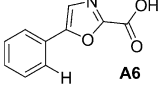
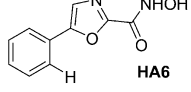
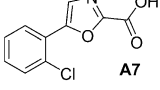
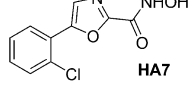
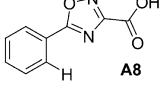
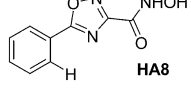
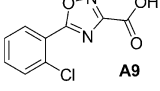
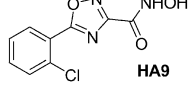
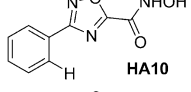
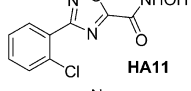
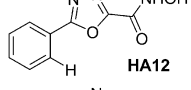
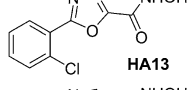
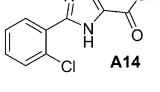
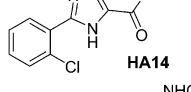
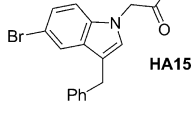
In the oxazole acid series, 2-aryl-oxazol-4-ylcarboxylic acids **A4** and **A5** appear as potent and selective inhibitors for the



Scheme 3. Synthesis of hydroxamic acids. *Reagents and conditions:* a) 1. $i\text{BuOCOC}$, Et_3N , THF , 0°C , 1 h, 2. NH_2OTBDMS , RT, 12 h, 3. TBAF, RT, 4 h; b) NH_2OK , MeOH , RT, 12 h.

Mn^{II} form of MetAP, with IC_{50} values in the micromolar range. These values are similar to those obtained for 5-arylfuran-2-yl-carboxylic acids used as standards in our assay conditions, as they were previously assayed against EcMetAP by Ye et al.^[16,17,38] Similarly, the unsubstituted phenyl derivative **A3** is less efficient, and the introduction of a substituent at the *ortho* position of the phenyl ring improves inhibitory potency. However, there is a significant influence of the relative positions of the aryl and acid substituents on the oxazole heterocycle: the 5-aryloxazol-2-ylcarboxylic acid regioisomers **A6** and **A7** are inefficient inhibitors. Moreover, 5-aryl-1,2,4-oxadiazol-3-ylcarboxylic acids **A8** and **A9** do not inhibit any form of EcMetAP. The imidazole acid **A14** is only moderately active against the Mn^{II} form.

Table 1. In vitro inhibition assays against *EcMetAP* loaded with Co^{II} , Fe^{II} , and Mn^{II} .

| Acids | Co^{II} | $\text{IC}_{50} [\mu\text{M}]^{[a]}$ Fe^{II} | Mn^{II} | Hydroxamic acids | Co^{II} | $\text{IC}_{50} [\mu\text{M}]^{[a]}$ Fe^{II} | Mn^{II} |
|---|-------------------------|---|-------------------------|--|-------------------------|---|-------------------------|
|  A1 | > 200 | 94 | 2.9 |  HA1 | 3.5 | 1 | 1.3 |
|  A2 | > 200 | > 200 | 1.5 |  HA2 | 5.7 | 1.3 | 1.4 |
|  A3 | > 200 | > 200 | 80 |  HA3 | 36 | 1.6 | 7.1 |
|  A4 | > 200 | > 200 | 4.5 |  HA4 | 4.8 | 1.2 | 1.8 |
|  A5 | > 200 | > 200 | 2.6 |  HA5 | 7.3 | 0.9 | 1.9 |
|  A6 | > 200 | > 200 | > 200 |  HA6 | 171 | 1.2 | 5.4 |
|  A7 | > 200 | > 200 | > 200 |  HA7 | 15.1 | 0.95 | 1.9 |
|  A8 | > 200 | > 200 | > 200 |  HA8 | 97 | 1.2 | 6.7 |
|  A9 | > 200 | > 200 | > 200 |  HA9 | 20.5 | 0.9 | 2 |
| | | | |  HA10 | > 200 | 1.3 | 30 |
| | | | |  HA11 | 36.5 | 1.15 | 7 |
| | | | |  HA12 | > 200 | 1.85 | 105 |
| | | | |  HA13 | 66 | 1 | 8.8 |
|  A14 | > 200 | > 200 | 62 |  HA14 | 40 | 2.35 | 4.9 |
| | | | |  HA15 | 5.2 | 1.0 | 2.8 |

[a] IC_{50} values represent the mean of three independent determinations with standard deviations < 20%.

As expected, hydroxamic acids are more potent inhibitors than the corresponding acids, regardless of the five-membered heterocycle being a furan, an oxazole, an oxadiazole, or an imidazole. Whereas with the most efficient molecules bearing a chloro or a trifluoromethyl group at the *ortho* position of the phenyl ring a complete loss of metalloform selectivity is observed, compounds with an unsubstituted phenyl ring—**HA6**, **HA8**, and **HA10**—display high selectivity for MetAP loaded with Mn^{II} and Fe^{II} versus Co^{II} . Meanwhile, the 5-phenyl-1,2,4-oxadiazol-2-ylhydroxamic acid **HA12** is highly selective for the Fe^{II} form over the Mn^{II} and Co^{II} forms, with an IC_{50} value for *EcMetAP-Fe* of 1.85 μM , which is 50- and 100-fold lower than for *EcMetAP-Mn* and *EcMetAP-Co*, respectively. Usually, the design of an inhibitor targeting a metalloprotease should involve a balance between the binding affinity at the metal active site and the strength of interactions of the peptide or non-peptide scaffold with amino acid residues of the protein backbone. However, in accordance with the specific involvement of siderophores in iron chelators,^[39] the hydroxamic moiety is a stronger chelator of iron than it is of manganese. To specifically target the iron metalloform, compounds with this binding group need not have very high affinity for the $\text{S1}'$ subsite, which interacts with the methionine side chain of MetAP substrates.

Finally, we tested some of our indole hydroxamic acids known as potent inhibitors of *EcPDF-Ni*. One of them, 2-(3-benzyl-5-bromoindol-1-yl)-*N*-hydroxyacetamide, **HA15** (**23c** in Ref. [24]; IC_{50} = 312 nM against *EcPDF-Ni*), appeared as active against *EcMetAP* as the most efficient hydroxamic acid described

above. This inhibitor is the first mixed inhibitor of EcPDF and EcMetAP.

X-ray crystal structures of EcMetAP-Mn in complex with HA5 and HA7 and structural model of EcMetAP-HA15

To gain insight into the positioning of the oxazole heterocycle with reversed substitutions at positions 2 and 5, we tried to solve the X-ray crystal structure of EcMetAP with two such regioisomers bearing a hydroxamic acid as chelating group. We obtained crystals of EcMetAP-Mn in complex with **HA5** and **HA7**. These crystallizations were carried out at an enzyme concentration of 0.4 mM and [metal]/[apo-MetAP] ratios of 1, 0.5, and 0.25 to favor the binding of a single divalent metal cation at the active site. Unexpectedly, the crystal structures are identical regardless of metal content, and the enzyme consistently has a dinuclear active site (Mn₁–Mn₂ distance: 3.4 Å) with metal ion occupancies of 100% for both sites. Structures solved at a [metal]/[apo-MetAP] ratio of 1 are shown in Figure 1a,b. The hydroxamate binds the two metal cations and adopts an (O,O) chelating mode to Mn₁ at the higher-affinity site, while the oxygen atom of the hydroxamate bridges the two metal cations. In the EcMetAP-HA5 complex, the bridging oxygen atom O₁ is roughly equidistant from the two Mn^{II} ions (Mn₁...O₁: 2.08 Å and Mn₂...O₁: 1.95 Å), whereas in the EcMetAP-HA7 complex the O₁–Mn₂ distance is significantly shorter than that of O₁–Mn₁ (Mn₁...O₁: 2.34 Å and Mn₂...O₁: 1.88 Å). In both complexes the carbonyl oxygen atom of the hydroxamic acid interacts weakly with Mn₁ (Mn₁...O₂: 2.36 and 2.33 Å for **HA5** and **HA7**, respectively).

In the holoenzyme active site, the coordination geometry of Mn₁ is distorted trigonal bipyramidal, whereas that of Mn₂ is distorted octahedral.^[37] In this active site, Asp108O^{δ1} and Glu204O^{ε2} occupy the axial positions of Mn₁, while O_{waterA}, His171N^{ε2} and Glu235O^{ε1} define the equatorial plane. The same O_{waterA} atom together with Asp108O^{δ2} and bidentate Asp97O^{δ1},O^{δ2} make up the equatorial plane of Mn₂, while Glu235O^{ε2} and another O_{waterB} are in axial position. Here, in both structures in the presence of **HA5** or **HA7**, binding of the inhibitors expands the coordination sphere of Mn₁ in a distorted

geometry. In addition, Asp97 rotates slightly, resulting in a lower O–Mn₂ interaction (Mn₂...Asp97 O^{δ2}: 2.79 and 2.68 Å for **HA5** and **HA7**, versus 2.4 Å in the holoenzyme). The carboxylate group of the aspartate residue is twisted toward the bridging NHO of the hydroxamate to promote the formation of a strong hydrogen bond with the NH moiety of this group. Interestingly, Asp97 adopts a binding mode between that observed in the free binuclear Mn^{II} enzyme (pure bidentate binding to Mn₂),^[8] and in the mononuclear Mn^{II} form complexed with a hydrazide (strong hydrogen bonding with the NHHN₂ of the hydrazide),^[9] see figure S1 in the Supporting Information).

Finally, the overall structure of inhibitors is not planar; the aromatic ring and the oxazole heterocycle are twisted (dihedral angles between the two cycles: 139° for **HA5** and 144° for **HA7**). In the two regioisomers, oxazole heteroatoms are both hydrogen bonded to the two histidines His178 and His79, which are highly conserved in all MetAP sequences. They are proposed to activate the bound water molecule and to participate in the orientation of the substrate.^[40,41] In **HA5** and **HA9** structures, it is always the nitrogen atom of the oxazole that is the closer to His178 (**HA5**: N...H178 3.43 Å, O...H178 5.50 Å; **HA7**: N...H178 2.88 Å, O...H178 4.52 Å), and the oxygen atom to

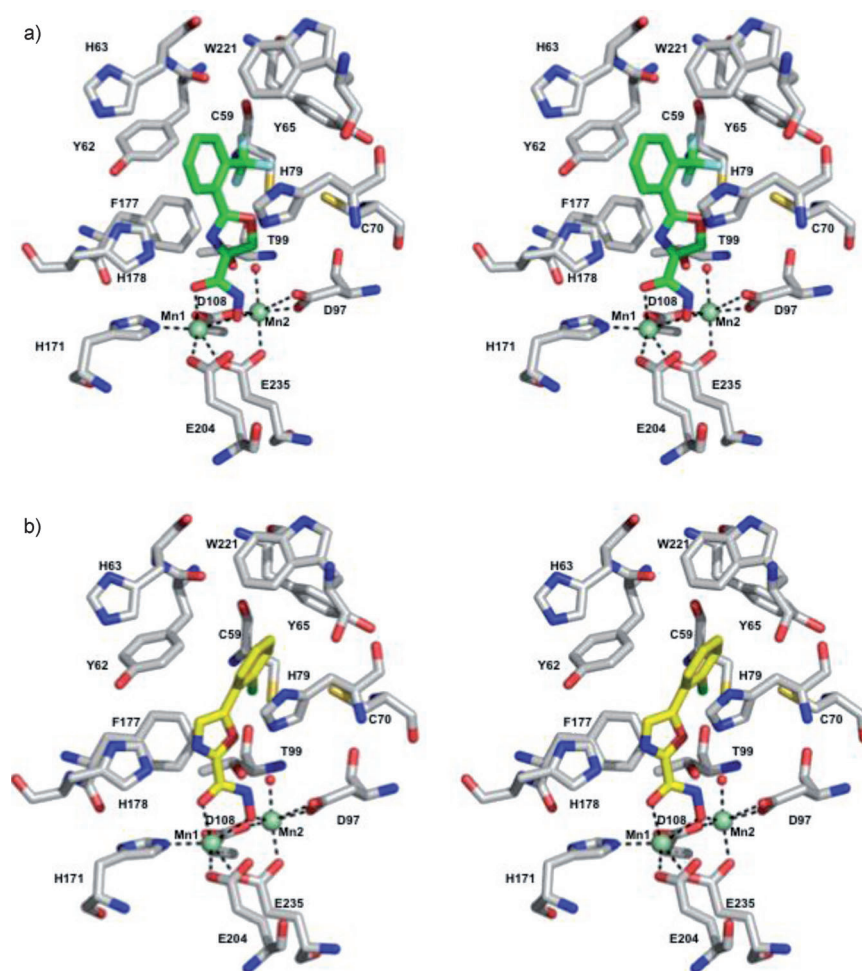


Figure 1. Stereo views of a) the **HA5**–EcMetAP-Mn complex and b) the **HA7**–EcMetAP-Mn complex; these structures correspond to crystals grown at a metal/apo-protein ratio of 1:1.

His79 (**HA5**: N...H79 4.27 Å, O...H79 3.45 Å; **HA7**: N...H79 5.52 Å, O...H79 3.83 Å). The selectivity of these hydrogen bonds might partly explain the differences in interactions of the hydroxamates **HA5** and **HA7** to the dinuclear active site. They could force **HA7** to interact more strongly with Mn₂ than with Mn₁.

The question that arises is the relevance of these structures in relation to the enzyme assay conditions. The fact that same structures are observed for both inhibitors at [metal]/[apo-MetAP] ratios of 0.5 and 0.25 supports a positive answer. The starting enzyme is likely to be mononuclear in the assays, but the inhibited form is dinuclear. This result may be consistent with a cooperative binding of the two metal cations, as previously proposed by Larrabee et al.^[11] and Holz and colleagues^[12] on the basis of spectroscopic data analyses. One hypothesis should be that hydroxamates bind a mononuclear form of MetAP, promoting an increase in the binding affinity for the second Mn center, and the final inhibited state of MetAP would be always dinuclear. Thus, the cooperative metal binding appears to be inhibitor-dependent.

We did not succeed in obtaining crystals of *Ec*MetAP-Mn in complex with the indole hydroxamic derivative **HA15** suitable for X-ray analysis, so we performed a molecular modeling study by replacing the oxazole **HA7** with **HA15** in the crystal structure (PDB ID: 4A6W). Both the indole and the phenyl rings are located deeply inside the S1' pocket, as shown in Figure 2.

Antibacterial activities

Supporting Information table S1 lists the results obtained on isogenic *E. coli* strains (AG100 and AG100A) in the presence and absence of sub-inhibitory concentrations of polymyxin B nonapeptide (PMBN used at 20% of its MIC value), a molecule known to increase membrane permeability.^[42] AG100 is a wild-type *E. coli* strain, and AG100A is the isogenic derivative strain, in which the efflux pump *acrAB* genes are deleted. Most of the MIC values are greater than 64 µg mL⁻¹. A small increase in susceptibility was observed in the presence of PMBN as permeabilizer; the most significant effect was observed with furan (**A1**, **HA1**, and **HA2**) and oxazole (**HA5** and **HA7**) derivatives. Additional experiments were conducted with **HA1**, **HA2**, **HA5**, and **HA7** (Table 2). To evaluate the role of other efflux pump systems present in *E. coli* that can limit the intracellular uptake of MetAP inhibitors, the activities of these compounds were tested on AG100A in the presence of PAβN, an efflux pump blocker, and of both PMBN and PAβN. A two- to eightfold decrease in MIC values was observed, indicating that as previously reported by us^[42] and others,^[14,43] both the low permeability of the outer membrane and the efficiency of efflux pumps limit the intracellular activity of such hydroxamic compounds in *E. coli*.

It is generally reported that antibacterial molecules are more active toward Gram-positive than Gram-negative bacteria, as the additional outer membrane of the latter organisms impedes uptake.^[44] We therefore decided to determine whether these MetAP inhibitors are active toward Gram-positive bacteria. All the compounds were tested against two Gram-positive strains, *Staphylococcus aureus* and *Enterococcus hirae*, but nei-

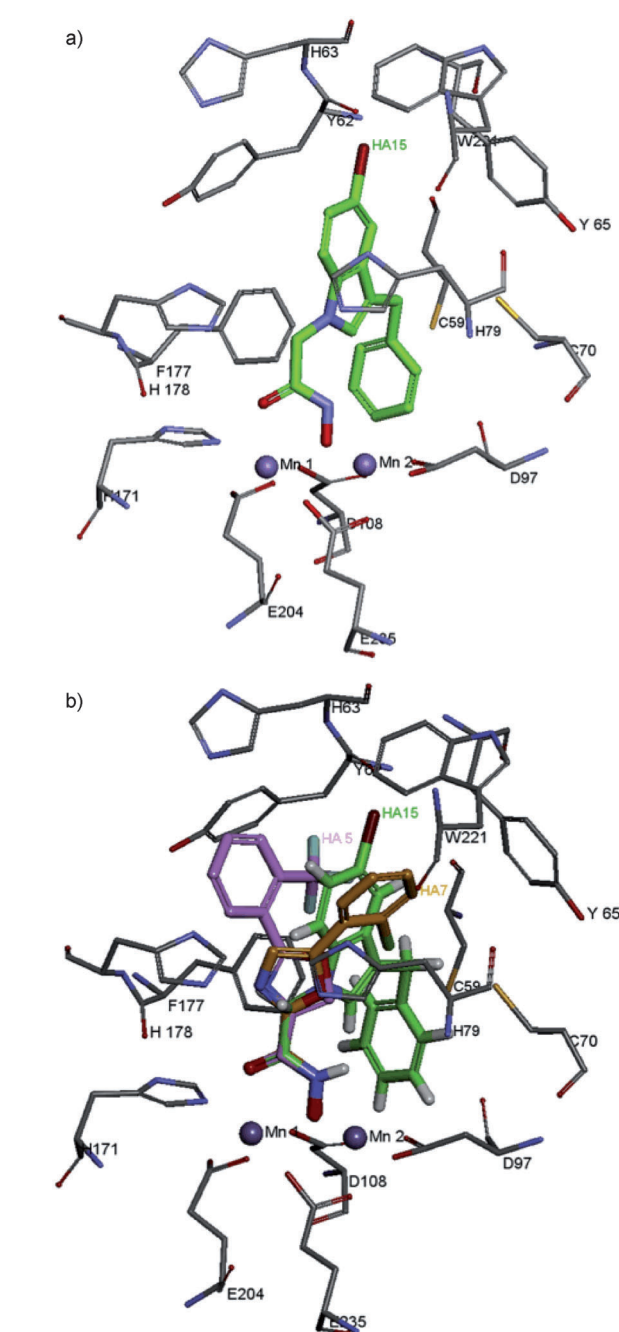


Figure 2. a) Representation of the **HA15**–*Ec*MetAP-Mn complex obtained after molecular dynamics and energy minimization. b) Superimposition of **HA5** (purple), **HA15** (green), and **HA7** (brown) inside the *Ec*MetAP-Mn structure.

ther were susceptible to the hydroxamic acids at low concentration (data not shown).

Conclusions

In this study the inhibitory potencies of a new series of hydroxamic acids attached to five-membered heterocycles substituted by an aryl group were evaluated against *Ec*MetAP loaded with Co^{II}, Mn^{II}, and Fe^{II}. In contrast to furan acids, which are selective for the Mn^{II} form, furan, oxazole, oxadiazole, and

Table 2. Activity of MetAP inhibitors on *E. coli* strains: effect of adjuvants.^[a]

| Conditions | MIC [$\mu\text{g mL}^{-1}$] | | | |
|------------------------------|-------------------------------|-------|-------|------|
| | HA1 | HA2 | HA5 | HA7 |
| AG100 | > 64 | > 64 | > 64 | > 64 |
| AG100 + PMBN | 16–8 | 64–32 | 64 | 64 |
| AG100A | 64 | 64 | 64 | 64 |
| AG100A + PMBN | 16 | 64–32 | 64 | 16 |
| AG100A + PA β N | 32 | 16–8 | 32–16 | 16 |
| AG100A + PMBN + PA β N | 16 | 8–4 | 32–16 | 8 |

[a] Values are the means of four independent assays; AG100 and AG100A are wild-type and *acrAB*[−] *E. coli* strains, respectively; PMBN permeabilizer used at 20% of its MIC value; PA β N: efflux pump blocker used at 20 $\mu\text{g mL}^{-1}$.

imidazole hydroxamic acids are selective for both the Mn^{II} and Fe^{II} forms. One compound, 5-phenyl-1,2,4-oxadiazol-2-ylhydroxamic acid **HA12**, is highly selective for the Fe^{II} form, with an IC₅₀ value of $1.85 \pm 0.15 \mu\text{M}$, which is 50- and 100-fold lower than those for the Mn^{II} and Co^{II} forms, respectively. However, despite significant activity toward an iron form, only the furanyl- and oxazolylhydroxamic acid bearing a 2-chloro or 2-trifluoromethylphenyl group as heterocycle substituent display a slight antibacterial activity against *acrAB*[−] *E. coli* strains. To get insight into the positioning of the heterocycle in the protein, X-ray crystal structures of EcMetAP-Mn in complex with two regioisomers of oxazole hydroxamic acids **HA5** and **HA7** were solved. They indicate that the heterocycle is anchored in the protein through strong hydrogen bonding interactions between the nitrogen and oxygen heteroatoms of the oxazole ring and the conserved His198 and His79 residues, respectively. Moreover, although the enzyme is likely to be mononuclear in enzyme assays with a [metal]/[apo-protein] ratio of 5, for EcMetAP-Mn-inhibitor complexes, the enzyme is consistently dinuclear when crystallized with Mn/apo-protein ratios of 1, 0.5, or 0.25, suggesting a cooperative metal binding mode. An indole hydroxamic acid has been identified as the first mixed EcPDF/EcMetAP inhibitor. All these results underscore the interest in hydroxamic acids, which are known to be capable of efficiently binding the mononuclear or dinuclear active sites of metalloproteins.

Experimental Section

Chemistry

All solvents and chemicals were purchased from SDS and Aldrich, respectively. DMF, THF, and CH₂Cl₂ were dried according to standard procedures. ¹H NMR and ¹³C NMR spectra were recorded on ARX-250 or Bruker Avance 500 spectrometers. Chemical shifts (δ) are expressed in ppm downfield from TMS. IR spectra were obtained with a PerkinElmer Spectrum One FTIR spectrometer equipped with a MIRacle single-reflection horizontal ATR unit (germanium crystal). ESI mass spectrometry analyses of small molecules were performed on a Thermo Finnigan LCD Advantage spectrometer. HRMS and elemental analyses were carried out by the microanalysis services at Gif-sur-Yvette (CNRS, France). ESIMS analyses of proteins were performed on an LTQ Orbitrap instrument at

the Cochin Institute of Paris Descartes University (France). The various synthetic pathways for the products are depicted in Schemes 1–3.

5-(2-Chlorophenyl)furan-2-carboxylic acid A1: An aqueous solution of NaNO₂ (414 mg, 6 mmol, 3 mL) was added to an aqueous solution of 2-chloroaniline (638 mg, 5 mmol) in concentrated aqueous HCl (4 N, 3 mL) at 0 °C under stirring; 20 min later an aqueous solution of 2-furanoic acid (560 mg, 5 mmol) in acetone (3 mL) and an aqueous solution of CuCl₂ (256 mg, 1.5 mmol, 3 mL) were added. The precipitate that formed after one day of stirring at room temperature was isolated to give **A1** as a brown powder (523 mg, 47%). ¹H NMR (250 MHz, CDCl₃): δ = 7.24 (d, ³J = 3.6 Hz, 1 H), 7.31 (d, ³J = 3.6 Hz, 1 H), 7.35 (td, ³J = 7.5 Hz, ⁴J = 1.7, 1 H), 7.42 (td, ³J = 7.5 Hz, ⁴J = 1.35 Hz, 1 H), 7.52 (dd, ³J = 7.5 Hz, ⁴J = 1.35 Hz, 1 H), 7.98 ppm (dd, ³J = 7.5 Hz, ⁴J = 1.35 Hz, 1 H); ¹³C NMR (500 MHz, CDCl₃): δ = 113.6, 120.5, 128.4, 129.6, 130.9, 131.8, 145.6, 154.6, 161.6, 129.2, 132 ppm; MS (ESI[−], MeOH) *m/z* (%): 220.9 (100) [M−H][−]; Anal. calcd for C₁₁H₇ClO₃: C 59.35, H 3.17, found: C 59.21, H 3.18.

5-(2-(Trifluoromethyl)phenyl)furan-2-carboxylic acid A2: Following a similar procedure as above, 256 mg of **A2** (20%) were obtained as a brown powder from 2-trifluoromethylaniline (0.805 g, 5 mmol). ¹H NMR (250 MHz, CD₃OD): δ = 6.83 (dq, ³J = 3.7 Hz, *J*_{HF} = 0.7 Hz, 1 H), 7.30 (d, ³J = 3.7 Hz, 1 H), 7.72 (t, ³J = 7.8 Hz, 1 H), 7.61 (t, ³J = 7.8 Hz, 1 H), 7.84 ppm (m, 2 H); ¹³C NMR (500 MHz, CD₃OD): δ = 113, 120.5, 133.5, 132, 130.5, 127.5 (*J*_{CF} = 5.4 Hz), 146.5, 155.5, 161.5, 128.5 (*J*_{CF} = 32 Hz), 125.3 (*J*_{CF} = 273.4 Hz), 129.5 ppm; MS (ESI[−], MeOH) *m/z* (%): 254.8 (100) [M−H][−]; Anal. calcd for C₁₂H₇F₃O₃: C 56.26, H 2.75, found: C 56.07, H 2.71.

2-Phenyloxazole-4-carboxylic acid A3: An aqueous solution of LiOH (2 m, 1 mL) was added to a suspension of **3a** in a mixture of H₂O (1 mL) and THF (200 μL). The mixture was stirred for 1 h, then acidified to pH 2 with HCl. This solution was extracted with EtOAc, and the organic layer was washed with brine and dried over MgSO₄. Evaporating the solvent yielded **A3** as a white solid (77 mg, 81%). ¹H NMR (250 MHz, [D₆]DMSO): δ = 7.59 (m, 3 H), 8.02 (m, 2 H), 8.86 (s, 1 H), 13.24 ppm (bs, 1 H); ¹³C NMR (500 MHz, [D₆]DMSO): δ = 126.5, 126.6, 129.6, 131.6, 134.8, 145.8, 161.5, 162.4 ppm; MS (ESI[−], MeOH) *m/z* (%): 188.1 (10) [M−H][−], 144.1 (100) [M−CO₂−H][−]; Anal. calcd for C₁₀H₇NO₃: C 63.49, H 3.73, N 7.40, found: C 63.33, H 3.71, N 7.32.

A4 and **A5** were obtained by using a similar procedure as described for **A3**.

2-(2-Chlorophenyl)oxazole-4-carboxylic acid A4: Compound **3a** (143 mg, 92%) was obtained as a white powder from **3b** (165 mg, 0.69 mmol). ¹H NMR (250 MHz, [D₆]DMSO): δ = 7.88 (m, 2 H), 8.0 (d, ³J = 7.5 Hz, 1 H), 8.05 (d, ³J = 7.5 Hz, 1 H), 9.0 (s, 1 H), 13.3 ppm (bs, 1 H); ¹³C NMR (250 MHz, CDCl₃): δ = 125.2, 126.9, 131.2, 131.6, 132.1, 133, 133.6, 145.2, 160.8, 164.9 ppm; Anal. calcd for C₁₀H₆ClNO₃: C 53.71, H 2.70, N 6.26, found: C 53.46, H 2.72, N 6.15.

2-(2-Trifluoromethylphenyl)oxazole-4-carboxylic acid A5: Compound **A5** (194 mg, 93%) was obtained as a brown powder from **3c** (220 mg, 0.81 mmol). ¹H NMR (250 MHz, [D₆]DMSO): δ = 7.88 (m, 2 H), 8.0 (m, 1 H), 8.05 (dd, ³J = 7.3 Hz, ⁴J = 1.5 Hz, 1 H), 8.96 ppm (s, 1 H); ¹³C NMR (250 MHz, CDCl₃): δ = 121.1, 124.7, 127.1, 128.6, 131.2, 132, 132.1, 133.8, 133.8, 145.8, 160.8, 164.7 ppm; Anal. calcd for C₁₁H₆F₃NO₃·0.2LiOH: C 50.43, H 2.38, N 5.34, found: C 50.64, H 2.46, N 5.31.

5-Phenyloxazole-2-carboxylic acid A6: Compound **A6** (76 mg, 94%) was obtained by saponification of **6a** (93 mg, 0.43 mmol)

with LiOH in a THF/H₂O mixture as described above for **A3**. ¹H NMR (250 MHz, [D₆]DMSO): δ = 7.50 (m, 3H), 7.81 (d, ³J = 7 Hz, 2H), 7.95 ppm (s, 1H); ¹³C NMR (250 MHz, [D₆]DMSO): δ = 117.3, 124.4, 129.0, 129.5, 131.5, 137.4, 151.3, 156.1 ppm; HRMS-ESI[−] *m/z* [M−H][−] calcd for C₁₀H₆NO₃[−]: 188.0348, found: 188.0350.

5-(2-Chlorophenyl)oxazole-2-carboxylic acid A7: Compound **A7** (104 mg, 82%) was obtained as a white powder from **6b** (150 mg, 0.6 mmol). ¹H NMR (250 MHz, [D₆]DMSO): δ = 7.53 (m, 2H), 7.67 (m, 1H), 7.87 (m, 1H), 8.02 (s, 1H), 8.58 ppm (bs, 1H); ¹³C NMR (250 MHz, [D₆]DMSO): δ = 119.2, 133.7, 137.9, 138.3, 139.2, 140.0, 143.1, 168.1, 172.4, 176.8 ppm; HRMS-ESI[−] *m/z* [M−H][−] calcd for C₁₀H₅³⁵ClNO₃[−]: 221.9958, found: 221.9953; Anal. calcd for C₁₀H₆ClNO₃: C 53.71, H 2.70, N 6.26, found: C 53.81, H 3.15, N 6.51.

5-Phenyl-1,2,4-oxadiazole-3-carboxylic acid A8: Compound **A8** (200 mg, 82%) was obtained as a white powder by saponification with LiOH in a THF/H₂O mixture of **9a** (217 mg, 1.06 mmol). ¹H NMR (500 MHz, [D₆]DMSO): δ = 7.67 (m, 2H), 7.56 (m, 1H), 8.16 ppm (d, ³J = 7.6 Hz, 1H); ¹³C NMR (500 MHz, [D₆]DMSO): δ = 124.9, 128.3, 129.7, 133.8, 154.7, 163.5, 176.9 ppm; MS (ESI[−], MeOH) *m/z* (%): 145.1 (100) [M−H−CO₂][−]; Anal. calcd for C₉H₆N₂O₃·0.5 LiCl·H₂O: C 47.13, H 3.52, N 12.21, found: C 47.05, H 3.67, N 12.05.

5-(2-Chlorophenyl)-1,2,4-oxadiazole-3-carboxylic acid A9: Compound **A9** (421 mg, 95%) was obtained as a white powder by saponification of **9b** (500 mg, 1.98 mmol) with LiOH/THF/H₂O. ¹H NMR (500 MHz, [D₆]DMSO): δ = 7.61 (m, 1H), 7.75 (m, 2H), 8.15 (d, ³J = 7.6 Hz, 1H); ¹³C NMR (500 MHz, [D₆]DMSO): δ = 124.1, 129.9, 133.3, 134.2, 136.5, 160.3, 164.6, 176.7 ppm; Anal. calcd for C₉H₅ClN₂O₃·0.1 H₂O: C 47.74, H 2.31, N 12.37, found: C 48.03, H 2.24, N 12.22.

5-(2-Chlorophenyl)-1H-imidazole-2-carboxylic acid A14: Compound **A14** was isolated as the hydrochloride salt (pink powder, 70% yield). ¹H NMR (250 MHz, CD₃OD): δ = 7.62 (td, ³J = 7.0 Hz, ⁴J = 2.3 Hz, 1H), 7.74 (m, 2H), 7.79 (d, ³J = 7.0 Hz, 1H), 8.28 ppm (s, 1H); ¹³C NMR (500 MHz, CD₃OD): δ = 124.22, 125.87, 128.45, 129.05, 131.87, 133.39, 134.68, 135.25, 145.51, 160.44 ppm; MS (ESI[−], MeOH) *m/z* (%): 221.4 (100) [M−H][−]; HRMS-ESI⁺ *m/z* calcd for C₁₀H₈N₂O₂³⁵Cl 223.0274, found: 223.0268; Anal. calcd for C₁₀H₈Cl₂N₂O₂·0.37 KCl: C 41.90, H 2.81, N 9.77, found: C 41.91, H 2.73, N 9.88.

Preparation of hydroxamic acids

Procedure A from the acid: Et₃N (0.54 mmol) and isobutylchloroformate (0.47 mmol) were added to a solution of the acid (0.45 mmol) in THF (10 mL) at 0 °C under argon. The solution was stirred for 1 h, then filtered under argon. *O*-(*tert*-Butyldimethylsilyl)-hydroxylamine (0.9 mmol) was added to the clear solution. The mixture was allowed to warm to room temperature and stirred overnight. A solution of TBAF in THF (1 M, 0.9 mmol) was added, and the solution was stirred for an additional 4 h. After evaporation of the solvent, the residue was dissolved in EtOAc, and the organic layer was washed with saturated aqueous NaHCO₃, then with 0.1 N HCl and brine. Once filtered, the solution was evaporated in vacuo.

Procedure B from the ester: A solution of NH₂OK was prepared as described previously by Huang et al.^[36] A suspension of NH₂OH·HCl (2.35 g, 34 mmol) in MeOH was held at reflux under argon. A solution of KOH (3.35 g, 50 mmol) in MeOH (7 mL) was added to the resulting clear solution. After holding at reflux for 30 min, the mixture was cooled and filtered to give a clear solution of NH₂OK esti-

mated to 1.75 M. NH₂OK in MeOH (4.2 mmol, 2.39 mL) was added to the ester (0.42 mmol) dissolved in MeOH (2 mL). The mixture was stirred overnight then acidified to pH 3–4 with 1 N HCl at 0 °C. The solution was diluted with EtOAc, washed with brine, dried over Na₂SO₄, filtered, and evaporated in vacuo.

5-(2-Chlorophenyl)-N-hydroxyfuran-2-carboxamide HA1: Compound **HA1** (27 mg, 40%) was obtained as a red powder from the acid **A1** (100 mg, 0.45 mmol) after purification over silica gel (eluent CH₂Cl₂/MeOH, 100:0→95:5). ¹H NMR (250 MHz, [D₆]acetone): δ = 7.23 (d, ³J = 3.5 Hz, 1H), 7.31 (d, ³J = 3.5 Hz, 1H), 7.45 (m, 2H), 7.58 (dd, ³J = 7.7 Hz, ⁴J = 1.5 Hz, 1H), 8.15 (dd, ³J = 7.7 Hz, ⁴J = 1.5 Hz, 1H), 8.36 (bs, 1H, NH), 10.8 ppm (bs, 1H, OH); ¹³C NMR (500 MHz, [D₆]DMSO): δ = 112.9, 115.9, 127.8, 128.4, 129.1, 130.0, 130.6, 131.2, 146.3, 151.7, 156.7 ppm; MS (ESI[−], MeOH) *m/z* (%): 236 (100) [M−H][−]; Anal. calcd for C₁₁H₉ClNO₃·0.4 CH₂Cl₂·0.2 H₂O: C 49.71, H 3.44, N 5.08, found: C 49.51, H 3.43, N 5.07.

N-Hydroxy-5-(2-(trifluoromethyl)phenyl)furan-2-carboxamide

HA2: Compound **HA2** (76 mg, 55%) was obtained as white needles after recrystallization from acetone/CH₂Cl₂ from the acid **A2** (130 mg, 0.51 mmol). ¹H NMR (250 MHz, [D₆]acetone): δ = 6.89 (d, ³J = 3.5 Hz, 1H), 7.22 (d, ³J = 3.5 Hz, 1H), 7.67 (t, ³J = 8 Hz, 1H), 7.79 (t, ³J = 7.5 Hz, 1H), 7.9 (d, ³J = 7.5 Hz, 1H), 7.98 (d, ³J = 8 Hz, 1H), 8.43 (bs, 1H, NH), 10.64 ppm (bs, 1H, OH); ¹³C NMR (500 MHz, [D₆]acetone): δ = 113.2, 116.7, 127.8, 130.7, 133.8, 132.2, 128.0 (*J*_{CF} = 6.3 Hz), 131.2, 148.2, 152.9, 157.9 ppm; MS (ESI[−], MeOH) *m/z* (%): 270.1 (100) [M−H][−]; Anal. calcd for C₁₂H₈F₃NO₃: C 53.15, H 2.97, N 5.16, found: C 52.85, H 2.99, N 5.08.

N-Hydroxy-2-phenyloxazole-4-carboxamide HA3: Starting from the acid **A3** (77 mg, 0.41 mmol), **HA3** (23 mg, 28%) was obtained as a white powder after recrystallization in a mixture of CH₂Cl₂/MeOH/cyclohexane 3:1:6. ¹H NMR (250 MHz, [D₆]acetone): δ = 7.57 (m, 3H), 8.05 (m, 2H), 8.35 (bs, 1H, NH), 8.48 (s, 1H), 10.61 ppm (bs, 1H, OH); ¹³C NMR (500 MHz, [D₆]acetone): δ = 127.7, 128, 130.4, 132.4, 137.2, 142.6, 159.3, 162.7. MS (ESI[−], MeOH) *m/z* (%): 203.1 (100) [M−H][−]; Anal. calcd for C₁₀H₈N₂O₃: C 58.82, H 3.95, N 13.72, found: C 58.39, H 4.01, N 13.56.

N-Hydroxy-2-(2-chlorophenyl)oxazole-4-carboxamide

HA4: Compound **HA4** (85 mg, 57%) was obtained as a white powder from the acid **A4** (142 mg, 0.63 mmol) after recrystallization in acetone/CH₂Cl₂. ¹H NMR (250 MHz, [D₆]acetone): δ = 7.85 (m, 2H), 7.98 (dd, ³J = 6.8 Hz, ⁴J = 2.0 Hz, 1H), 8.09 (d, ³J = 6.8 Hz, 1H), 8.35 (bs, 1H, NH), 8.62 (s, 1H), 10.54 ppm (bs, 1H, OH); ¹³C NMR (500 MHz, [D₆]acetone): δ = 122.5, 126.3, 128, 132.5, 133.6, 137, 143.5, 158.8, 160.4 ppm; Anal. calcd for C₁₀H₇ClN₂O₃: C 50.33, H 2.96, N 11.74, found: C 50.15, H 2.77, N 11.30.

N-Hydroxy-2-(2-trifluoromethylphenyl)oxazole-4-carboxamide

HA5: Compound **HA5** (239 mg, 53%) was obtained as a beige solid from the acid **A5** (226.7 mg, 0.88 mmol) after recrystallization in acetone/CH₂Cl₂. ¹H NMR (250 MHz, [D₆]acetone): δ = 7.44 (m, 3H), 8.05 (dd, ³J = 7.3 Hz, ⁴J_{HF} = 2.0 Hz, 1H), 8.36 (bs, 1H, NH), 8.44 (s, 1H), 10.47 ppm (bs, 1H, OH); ¹³C NMR (500 MHz, [D₆]acetone): δ = 107.7, 109.4, 128, 129.7, 133.5, 133.7, 134.6, 138.1, 144.1, 160.2, 161.7 ppm; MS (ESI[−], MeOH) *m/z* (%): 271 (100) [M−H][−]; Anal. calcd for C₁₁H₇N₂F₃O₃: C 48.54, H 2.59, N 10.29, found: C 48.22, H 2.43, N 10.11.

N-Hydroxy-5-phenyloxazole-2-carboxamide HA6: The final product prepared from the acid **A6** (54 mg, 0.29 mmol) was solubilized in a minimal amount of acetone and isolated as a white powder upon precipitation in pentane (22 mg, 38%). ¹H NMR (250 MHz, [D₆]acetone): δ = 7.52 (m, 3H), 7.72 (s, 1H), 7.87 (d, ³J = 6.8 Hz, 2H),

8.64 (s, 1H), 10.96 ppm (s, 1H); ^{13}C NMR (500 MHz, $[\text{D}_6]\text{acetone}$): δ = 124.3, 126, 128.4, 130.3, 130.7, 154.3, 155, 155.5 ppm; MS (ESI^- , MeOH) m/z (%): 203 (100) $[\text{M}-\text{H}]^-$; Anal. calcd for $\text{C}_{10}\text{H}_8\text{N}_2\text{O}_3$: C 58.82, H 3.95, N 13.72, found: C 58.85, H 4.08, N 13.01.

N-Hydroxy-5-(2-chlorophenyl)oxazole-2-carboxamide HA7: The final product prepared from the acid **A7** (80 mg, 0.36 mmol) was solubilized in a minimal amount of acetone and isolated as a white powder upon precipitation in pentane (14 mg, 16%). ^1H NMR (250 MHz, $[\text{D}_6]\text{DMSO}$): δ = 7.55 (m, 2H), 7.68 (m, 1H), 7.99 (s, 1H), 8.01 (m, 1H), 9.56 (s, 1H), 11.93 ppm (s, 1H); ^{13}C NMR (500 MHz, $[\text{D}_6]\text{acetone}$): δ = 127.1, 128.7, 128.9, 129.9, 131.7, 132, 132.4, 151.5, 154.3, 155.3 ppm; MS (ESI^- , MeOH) m/z (%): 237 (100) $[\text{M}-\text{H}]^-$; Anal. calcd for $\text{C}_{10}\text{H}_7\text{ClN}_2\text{O}_3$: C 50.33, H 2.96, N 11.74, found: C 50.39, H 3.13, N 11.34.

N-Hydroxy-5-phenyl-1,2,4-oxadiazole-3-carboxamide HA8: Compound **HA8** (24 mg, 25%) was obtained as a white powder from the acid **A8** (90 mg, 0.47 mmol) after recrystallization in CH_2Cl_2 . ^1H NMR (500 MHz, $[\text{D}_6]\text{acetone}$): δ = 7.68 (t, 3J = 7.5 Hz, 2H), 7.75 (t, 3J = 7.5 Hz, 1H), 8.19 ppm (d, 3J = 7.5 Hz, 1H); ^{13}C NMR (500 MHz, $[\text{D}_6]\text{acetone}$): δ = 124.9, 129.5, 130.9, 134.9, 155.2, 164.6, 177.8 ppm; MS (ESI^- , MeOH) m/z (%): 204.1 (100) $[\text{M}-\text{H}]^-$; Anal. calcd for $\text{C}_9\text{H}_7\text{N}_3\text{O}_3$: C 52.69, H 3.44, N 20.48, found: C 52.68, H 3.46, N 20.31.

N-Hydroxy-5-(2-chlorophenyl)-1,2,4-oxadiazole-3-carboxamide HA9: The final product (88 mg, 62%) prepared from the ester **8b** (150 mg, 0.59 mmol) was isolated as a white powder upon precipitation from acetone into cold pentane. ^1H NMR (500 MHz, $[\text{D}_6]\text{DMSO}$): δ = 7.63 (m, 1H), 7.75 (m, 2H), 8.14 (d, 3J = 7.6 Hz, 1H), 9.66 (s, 1H), 11.87 ppm (s, 1H); ^{13}C NMR (500 MHz, $[\text{D}_6]\text{DMSO}$): δ = 124.1, 129.9, 133.2, 134.2, 134.3, 136.5, 155.4, 164.8, 176.3 ppm; MS (ESI^- , MeOH) m/z (%): 237.9, (100) $[\text{M}-\text{H}]^-$; Anal. calcd for $\text{C}_9\text{H}_6\text{ClN}_3\text{O}_3 \cdot 0.1\text{H}_2\text{O}$: C 44.77, H 2.58, N 17.4, found: C 44.23, H 2.54, N 16.95.

N-Hydroxy-3-phenyl-1,2,4-oxadiazole-5-carboxamide HA10: Starting from the ester **12a** (120 mg, 0.55 mmol), **HA10** (32 mg, 28%) was isolated as a white powder after purification over silica gel (eluent $\text{CH}_2\text{Cl}_2/\text{MeOH}/\text{cyclohexane}$ 3:1:6). ^1H NMR (250 MHz, $[\text{D}_6]\text{DMSO}$): δ = 7.63 (m, 3H), 8.08 (dd, 3J = 6.5 Hz, 4J = 1.5 Hz, 2H), 9.94 (s, 1H), 12.35 ppm (s, 1H); ^{13}C NMR (500 MHz, CD_3OD): δ = 127.4, 128.6, 130.3, 133.0, 153.1, 169.8, 170.2 ppm; MS (ESI^- , MeOH) m/z (%): 204.1 (100) $[\text{M}-\text{H}]^-$; HRMS- ESI^- m/z $[\text{M}-\text{H}]^-$ calcd for $\text{C}_9\text{H}_6\text{N}_3\text{O}_3^-$: 204.0409, found: 204.0414.

N-Hydroxy-3-(2-chlorophenyl)-1,2,4-oxadiazole-5-carboxamide HA11: Starting from the ester **12b** (100 mg, 0.40 mmol), **HA11** (92 mg, 92%) was isolated as a white powder after precipitation from acetone into cold pentane. ^1H NMR (500 MHz, $[\text{D}_6]\text{DMSO}$): δ = 7.58 (t, 3J = 7.8 Hz, 1H), 7.66 (t, 3J = 7.8 Hz, 1H), 7.72 (d, 3J = 7.8 Hz, 1H), 7.95 (d, 3J = 7.8 Hz, 1H), 9.94 (s, 1H), 12.29 ppm (s, 1H); ^{13}C NMR (500 MHz, $[\text{D}_6]\text{DMSO}$): δ = 124.7, 127.7, 130.8, 131.8, 132.1, 132.9, 150.2, 166.7, 168 ppm; MS (ESI^- , MeOH) m/z (%): 238.2 (100) $[\text{M}-\text{H}]^-$, 476.9 (100) $[2\text{M}-\text{H}]^-$; HRMS- ESI^- m/z $[\text{M}-\text{H}]^-$ calcd for $\text{C}_9\text{H}_5^{35}\text{ClN}_3\text{O}_3^-$: 238.0019, found: 238.0019.

N-Hydroxy-5-phenyl-1,3,4-oxadiazole-2-carboxamide HA12: Compound **HA12** (27 mg, 85%) prepared from the ester **14a** (50 mg, 0.21 mmol) was isolated as a white powder upon precipitation from CH_2Cl_2 into pentane. ^1H NMR (500 MHz, $[\text{D}_6]\text{DMSO}$): δ = 7.67 (m, 3H), 8.09 (d, 3J = 7, 2H), 9.74 (s, 1H), 12.15 ppm (s, 1H); ^{13}C NMR (500 MHz, $[\text{D}_6]\text{DMSO}$): δ = 122.7, 126.9, 129.4, 132.5, 150.7, 157.4, 164.7 ppm; MS (ESI^- , MeOH) m/z (%): 204.1 (100) $[\text{M}-\text{H}]^-$; HRMS- ESI^- m/z $[\text{M}-\text{H}]^-$ calcd for $\text{C}_9\text{H}_6\text{N}_3\text{O}_3^-$: 204.0409, found: 204.0403.

N-Hydroxy-5-(2-chlorophenyl)-1,3,4-oxadiazole-2-carboxamide

HA13: Compound **HA13** (29 mg, 54%) prepared from the ester **14b** (53.5 mg, 0.22 mmol) was isolated as a white powder upon precipitation from CH_2Cl_2 into pentane. ^1H NMR (250 MHz, $[\text{D}_6]\text{DMSO}$): δ = 7.7 (m, 3H), 8.07 (d, 3J = 7.5 Hz, 1H), 9.8 (s, 1H), 12.2 ppm (s, 1H); ^{13}C NMR (250 MHz, $[\text{D}_6]\text{acetone}$): δ = 122.6, 127.7, 131.3, 131.6, 132.9, 133.4, 151.1, 157.8, 163.6 ppm; MS (ESI^- , MeOH) m/z (%): 238 (100) $[\text{M}-\text{H}]^-$; Anal. calcd for $\text{C}_9\text{H}_6\text{ClN}_3\text{O}_3 \cdot 0.15\text{H}_2\text{O}$: C 44.6, H 2.62, N 17.34, found: C 44.75, H 2.56, N 17.11.

N-Hydroxy-5-(2-chlorophenyl)-1H-imidazole-2-carboxamide

HA14: Compound **HA14** (74 mg, 50%) prepared from the acid **A14** (80 mg, 0.36 mmol) was isolated as a pink powder. ^1H NMR (250 MHz, $[\text{D}_6]\text{acetone}$): δ = 7.53 (t, 3J = 7.5 Hz, 1H), 7.59 (t, 3J = 7.0 Hz, 1H), 7.66 (d, 3J = 7.5 Hz, 1H), 7.79 (dd, 3J = 7.5 Hz, 4J = 1.5 Hz, 1H), 8.01 (s, 1H), 10.29 (bs, 1H), 10.95 ppm (bs, 1H); ^{13}C NMR (500 MHz CD_3OD): δ = 121.5, 124.3, 128.9, 129.2, 131.9, 133.5, 134.7, 135.2, 145.1, 157.8 ppm; MS (ESI^- , MeOH) m/z (%): 236 (100) $[\text{M}-\text{H}]^-$; HRMS- ESI^+ m/z calcd for $\text{C}_{10}\text{H}_8\text{N}_3\text{O}_2^{35}\text{Cl}$ 238.0383, found: 238.0382; Anal. calcd for $\text{C}_{10}\text{H}_8\text{ClN}_3\text{O}_2 \cdot 1.4\text{KCl} \cdot 1.5\text{H}_2\text{O}$: C 29.62, H 2.98, N 10.36, found: C 29.85, H 2.74, N 10.58.

Protein purification and enzymatic assays

Purification of apo-EcMetAP (pET28) for enzyme assays: The expression plasmid for EcMetAP (pET28b-EcMetAP) was a kind gift from Prof. J. Larrabee (Middlebury College, VT, USA), Dr. W. T. Lowther (Howard Hughes Medical Institute, University of Oregon, USA), and Prof. B. W. Matthews (Wake Forest University School of Medicine, Winston-Salem, NC, USA). EcMetAP was purified as the apo-enzyme using the previously described protocol of Lowther et al.,^[45] with some minor modifications as described, such as the use of the detergent Bugbuster 1 \times instead of Triton X-100. The purity of the purified apo-enzyme was assessed by capillary electrophoresis (Experion, Bio-Rad) as $\geq 95\%$. The molecular mass of purified apo-MetAP was 29634.27 Da as determined by ESIMS on an LTQ Orbitrap instrument, in good agreement with the theoretical value.

Purification of apo-EcMetAP (pET23) for crystallization: The open reading frame for EcMetAP was amplified by PCR from the pXL1071 plasmid,^[46] kindly provided by Dr. Meinel (ISV, CNRS Gif-sur-Yvette, France) and subcloned into the Novagen pET23a vector using NdeI and EcoRI restriction sites. BL21(DE3) *E. coli* cells containing the expression plasmid pET23a-EcMetAP were grown in Luria-Bertani (LB) medium supplemented with ampicillin (100 $\mu\text{g mL}^{-1}$) at 37°C until OD_{600} reached 0.5–0.6. Expression of EcMetAP was induced by adding 0.3 mM isopropyl- β -D-thiogalactoside (IPTG) for 3 h at 30°C. Cells were pelleted and stored at -40°C until use. Cell pellets were thawed in buffer [50 mM HEPES (pH 7.5), 150 mM KCl, 15 mM methionine, 5 mM EDTA, lysozyme (0.2 mg mL^{-1}), 0.1% Triton X-100] at 10 mL (g pellet) $^{-1}$ and sonicated with a Vibra-cell sonicator (Fisher Bioblock, Vibra-Cell 75115, 500W) at 30% amplitude by two cycles of 1 min 15 s (3 s on, 15 s off) on ice. After centrifugation at 18000 rpm (37600 g) for 30 min, the clarified supernatant was subjected to ammonium sulfate precipitation (0 \rightarrow 55 \rightarrow 80%) and centrifuged (10000 rpm; 12000 g) for 30 min at 4°C. The C80 pellet was resuspended in 5 mL buffer [20 mM Tris-HCl (pH 7.4), 15 mM methionine, 5 mM EDTA] and dialyzed overnight against buffer A [20 mM Tris-HCl (pH 7.4), 15 mM methionine, 0.1 mM EDTA] followed by two buffer changes. The following day, the dialysate was loaded onto a HiLoad 16/10 Q-Sepharose column (GE Healthcare) equilibrated with buffer A, and

the sample was eluted with a linear NaCl gradient (0.2 m h^{-1} , 2.5 mL min^{-1}). After analysis by capillary electrophoresis (Experion, Bio-Rad), fractions from the main peak (containing EcMetAP) were pooled and concentrated to 5 mL by ultrafiltration (Amicon Ultra-15, Millipore). The sample was then further fractionated with a HiLoad 16/60 Superdex-75 column (GE Healthcare) equilibrated with chelexed buffer [25 mM HEPES (pH 7.5), 150 mM KCl, 15 mM methionine]. The purified apo-protein was dialyzed against the chelexed buffer for two more days, concentrated to 48 mg mL^{-1} , frozen with liquid nitrogen, and stored at -80°C . Typical yields were 30 mg L^{-1} of culture. The molecular mass of the purified apo-EcMetAP was 29 194.99 Da as determined by ESIMS on an LTQ Orbitrap mass spectrometer, in agreement with the theoretical value of 29 199.6 Da.

Inhibition assays: The apo-protein was washed free of methionine using chelexed activity buffer [25 mM HEPES (pH 7.5), 150 mM KCl] prior to all kinetics assays and refrozen until use. Just before the assay, the apo-enzyme was activated by the addition of divalent metal chloride salt (5 equiv) to $60 \mu\text{M}$ apo-enzyme for 10 min at room temperature. Activations with Fe^{II} were performed under anaerobic conditions under an inert atmosphere (glove box). A direct spectrophotometric assay was used as described by Mitra et al.^[47] The methionine *para*-nitroanilide substrate (Met-*p*NA) was purchased from Bachem Bioscience. The hydrolysis of Met-*p*NA was monitored continuously at 30°C by following the increase in absorbance of *p*NA at $\lambda 405 \text{ nm}$ for 10–30 min on a 96-well UV-star microplate (Greiner) and microplate spectrophotometer (Powerwave XS, Biotek). A typical inhibition assay contained activity buffer [25 mM HEPES (pH 7.5), 150 mM KCl, 0.4 mM Met-*p*NA, $15 \mu\text{M}$ metal(II) chloride (or $15 \mu\text{M}$ $\text{FeCl}_2 + 30 \mu\text{M}$ sodium ascorbate)], activated enzyme diluted 20-fold, inhibitor at various concentrations, and 1.5% DMSO. The enzyme assay with iron(II) was performed aerobically in the presence of sodium ascorbate as described by Wang et al.^[43] IC_{50} values were calculated by nonlinear regression analysis of the normalized activity (ratio of initial rates with or without inhibitor) against $\log[\text{inhibitor concentration}]$.

Crystallization and data collection

Initial crystallization conditions were determined using Crystal Screen and Index kits in 96-well sitting-drop plates (Hampton Research) at 293 K. Final crystals were obtained independently at 293 K by the sitting-drop vapor diffusion method from 2 μL drops. Inhibitors (**HA5** and **HA7**) were added to concentrated enzyme (12.75 mg mL^{-1}) at an inhibitor/enzyme ratio of 5:1. Mixtures of protein–inhibitor complexes were incubated for 5 min with MnCl_2 at various metal/enzyme ratios (1:1; 0.5:1; 0.25:1). Drops enclosed 1 μL protein solution mixed with 1 μL precipitant solution containing either 17–25% PEG 8000 and 100 mM HEPES buffer (pH 7.5) for samples involving **HA5** inhibitor, or 15–22% PEG 20000, 100 mM MES buffer (pH 6.5) for samples involving **HA7**. Crystals were transferred to the mother liquor containing 10% glycerol prior to flash freezing in liquid nitrogen. X-ray diffraction data from different crystals were collected on the ID29 ESRF (Grenoble, France) or PROXIMA1 SOLEIL (St. Aubin, France) beamlines and were processed using MOSFLM^[48] and SCALA.^[49] The crystals belong to the $P2_1$ space group for crystals involving **HA7** and **HA5**, with one and two molecule(s) per asymmetric unit respectively. Cell parameters and data collection statistics are reported in Table 3.

Structure solution and refinement: Structures, at a metal/enzyme ratio of 1:1, were solved at a resolution of 1.5 Å by single anomalous diffraction (SAD). The CCP4i program was used to find struc-

Table 3. X-ray data collection and refinement statistics.

| Parameters | HA5 | HA7 |
|---|-------------------------|-------------------------|
| <i>Data collection</i> | | |
| Space group | $P2_1$ | $P2_1$ |
| PDB ID | 4A6V | 4A6W |
| Metal ion | Mn^{II} | Mn^{II} |
| Unit cell parameters | | |
| a [Å] | 53.2 | 39.3 |
| b [Å] | 61.2 | 62.9 |
| c [Å] | 77.8 | 52.6 |
| α, β, γ [°] | 90, 107.6, 90 | 90, 109.4, 90 |
| Resolution [Å] | 37.06–1.46 | 31.25–1.46 |
| Outer resolution shell [Å] | 1.54–1.46 | 1.57–1.46 |
| No. reflections (obsd, unique) | 323 041, 80 700 | 151 827, 38 522 |
| Completeness [%] ^[a] | 98.3 (97.3) | 97.9 (96.2) |
| Multiplicity ^[a] | 4.0 (4.0) | 3.9 (3.9) |
| $I/\sigma(I)$ ^[a] | 7.1 (3.4) | 8.5 (4.7) |
| R_{merge} [%] ^[a,b] | 9.3 (27.5) | 8.1 (21.6) |
| <i>Refinement:</i> | | |
| Reflections (working, test) | 76 648, 5569 | 36 995, 2545 |
| R [%] ^[a] | 16.2 | 15.6 |
| R_{free} [%] ^[a] | 22.3 | 22.6 |
| <i>RMSD:</i> | | |
| Bond length [Å] | 0.022 | 0.022 |
| Bond angle [°] | 1.978 | 1.974 |
| B -factor [Å ²] | 19.7 | 16.4 |
| <i>Ramachandran statistics:</i> | | |
| Most favored [%] | 96.6 | 95.8 |
| Allowed [%] | 3.4 | 4.28 |

[a] Outer shell. [b] $R_{\text{merge}} = \sum_i \sum_h |I_{hi} - \langle I_h \rangle| / \sum_i \sum_h I_{hi}$, for which I_{hi} is the i^{th} observation of the reflection h , and $\langle I_h \rangle$ is the mean intensity of reflection h . [c] $R_{\text{factor}} = \sum ||F_o| - |F_c|| / \sum |F_o|$; R_{free} was calculated with a set of randomly selected reflections (5%).

tural solutions.^[50] Structures were achieved with the MOLREP program using an available *E. coli* MetAP structure (PDB ID: 2MAT)^[51] as the search model. The model was fully refined and completed from the data using REFMAC software.^[52] Refinement statistics are listed in Table 3. All residues fall in favorable regions of the Ramachandran plot. Selected bond distances are listed in table S2 (Supporting Information). All protein structure images were generated with PyMOL.^[52]

Bacterial strains

Strains used in this study: Briefly, *E. coli* K-12 AG100 strain (*argE3 thi-1 rpsL xyl mtl Δ (gal-uvrB) supE44*), AG100A (*acrAB*[−]) derivatives have been described elsewhere.^[42]

Antibiotic susceptibility tests: Bacteria were grown in Müller–Hinton (MH) broth at 37°C . Susceptibilities to MetAP inhibitors, polymyxin B nonapeptide (PMBN), phenylalanine–arginine– β -naphthylamide (PA β N), norfloxacin, and chloramphenicol were determined by the broth dilution method as previously described.^[42] Minimal inhibitory concentrations (MICs) were determined with an inoculum of 106 CFU in 1 mL MH broth containing twofold serial dilutions of each antibiotic. Isolates were classified as susceptible, intermediately susceptible, or resistant to the antibiotics tested according to the Antibiogram Committee of the French Society for Microbiology ([http://www.sfm-microbiologie.org/pages/?page=746&id_page=182]). For combination assays, serial dilutions of

tested molecules were incubated in the presence of the PMBN at 10 or 20% of MICs previously determined. Norfloxacin and chloramphenicol belonging to unrelated structural antibiotic groups were used as internal standards. The results were scored after 18 h at 37 °C and are expressed as $\mu\text{g mL}^{-1}$ (MIC).

Supporting Information

Synthesis and characterization of all intermediates are detailed: table S1: activity of MetAP inhibitors on *E. coli* strains; table S2: selected bond angles and distances in the EcMetAP-Mn-inhibitor complexes; figure S1: comparison of ligands binding at the free EcMetAP-Mn active site under its dinuclear (A) and mononuclear (D) forms with those observed in EcMetAP-Mn complexed with HA5 (B) and HA7 (C); figure S2: surface view from X-ray structure of EcMetAP-HA7.

Acknowledgements

We thank Prof. J. Larrabee (Middlebury College, VT, USA), Dr. W. T. Lowther (Howard Hughes Medical Institute, University of Oregon, USA), and Prof. B. W. Matthews (Wake Forest University School of Medicine, Winston-Salem, NC, USA) for the kind gift of the expression plasmid for EcMetAP (pET28b-EcMetAP), Dr. T. Meinnel (ISV, CNRS Gif-sur-Yvette, France) for the plasmid (pXL1071) used in crystallization assays, and Dr. C. Léon (UMR 8601, Université Paris Descartes PRES Paris Cité, France) for molecular modeling studies. This work was supported by the CNRS (France) and Paris Descartes University, and by Aix-Marseille University and IRBA. F.H. received a PhD fellowship from Research Ministry and L.M. a post-doctoral fellowship from ANR-2010 BLAN METABACT.

Keywords: antibacterial agents • hydroxamic acids • inhibitors • methionine aminopeptidase • X-ray structures

- [1] C. Giglione, C. A. Boularot, T. Meinnel, *Cell. Mol. Life Sci.* **2004**, *61*, 1455–1474.
- [2] S. Y. Chang, E. C. McGary, S. Chang, *J. Bacteriol.* **1989**, *171*, 4071–4072.
- [3] C. G. Miller, A. M. Kukral, J. L. Miller, N. R. Movva, *J. Bacteriol.* **1989**, *171*, 5215–5217.
- [4] C. T. Supuran, A. Scozzafava, B. W. Clare, *Med. Res. Rev.* **2002**, *22*, 329–372.
- [5] V. M. D'Souza, B. Bennett, A. J. Copik, R. C. Holz, *Biochemistry* **2000**, *39*, 3817–3826.
- [6] V. M. D'Souza, S. I. Swierczek, N. J. Cosper, L. Meng, S. Ruebush, A. J. Copik, R. A. Scott, R. C. Holz, *Biochemistry* **2002**, *41*, 13096–13105.
- [7] N. J. Cosper, V. M. D'Souza, R. Scott, R. C. Holz, *Biochemistry* **2001**, *40*, 13302–13309.
- [8] Q.-Z. Ye, S.-X. Xie, Z.-Q. Ma, M. Huang, R. P. Hanzlik, *Proc. Natl. Acad. Sci. USA* **2006**, *103*, 9470–9475.
- [9] M. Huang, S.-X. Xie, Z.-Q. Ma, Q.-Q. Huang, F.-J. Nan, Q.-Z. Ye, *J. Med. Chem.* **2007**, *50*, 5735–5742.
- [10] X. V. Hu, X. Chen, K. C. Han, A. S. Mildvan, O. Jun, J. O. Liu, *Biochemistry* **2007**, *46*, 12833–12843.
- [11] J. A. Larrabee, C. H. Leung, R. Moore, T. Thamrong-Nawasawat, B. H. Wessler, *J. Am. Chem. Soc.* **2004**, *126*, 12316–12324.
- [12] S. Mitra, K. M. Job, L. Meng, B. Bennett, R. C. Holz, *FEBS J.* **2008**, *275*, 6248–6259.
- [13] V. M. D'Souza, R. C. Holz, *Biochemistry* **1999**, *38*, 11079–11085.
- [14] S. C. Chai, W. L. Wang, Q.-Z. Ye, *J. Biol. Chem.* **2008**, *283*, 26879–26885.
- [15] S. C. Chai, Q.-Z. Ye, *Bioorg. Med. Chem. Lett.* **2010**, *20*, 2129–2132.
- [16] Q.-Z. Ye, S.-X. Xie, M. Huang, W.-J. Huang, J.-P. Lu, Z.-Q. Ma, *J. Am. Chem. Soc.* **2004**, *126*, 13940–13941.
- [17] Q.-Q. Huang, M. Huang, F.-J. Nan, Q.-Z. Ye, *Bioorg. Med. Chem. Lett.* **2005**, *15*, 5386–5391.
- [18] C. J. Marmion, D. Griffith, K. D. Nolan, *Eur. J. Inorg. Chem.* **2004**, 3003–3016.
- [19] E. M. F. Muri, M. J. Nieto, R. D. Sindelar, J. S. Williamson, *Curr. Med. Chem.* **2002**, *9*, 1631–1653.
- [20] A. Sharma, G. K. Khuller, S. Sharma, *Expert Opin. Ther. Targets* **2009**, *13*, 753–765.
- [21] B. Chevrier, H. D'Orchymont, C. Schalk, C. Tarnus, D. Moras, *Eur. J. Biochem.* **1996**, *237*, 393–398.
- [22] S. Benini, W. R. Rypniewski, K. S. Wilson, S. Miletti, S. Ciurli, S. Mangani, *J. Biol. Inorg. Chem.* **2000**, *5*, 110–118.
- [23] A. Boularot, C. Giglione, S. Petit, Y. Duroc, R. Alves de Sousa, V. Larue, T. Cresteil, F. Dardel, I. Artaud, T. Meinnel, *J. Med. Chem.* **2007**, *50*, 10–20.
- [24] S. Petit, Y. Duroc, V. Larue, C. Giglione, C. Leon, C. Soulama, A. Denis, F. Dardel, T. Meinnel, I. Artaud, *ChemMedChem* **2009**, *4*, 261–275.
- [25] A. J. Phillips, Y. Uto, P. Wipf, M. J. Reno, D. R. Williams, *Org. Lett.* **2000**, *2*, 1165–1168.
- [26] G. Ernst, W. Fietze, R. Jacobs, E. Phillips (AstraZeneca), Nicotinic Acetylcholine Receptor Ligands, Int. Pat. WO/2005061510 (A1), **2005**.
- [27] R. N. Patel, L. Chu, R. Chidambaram, J. Zhu, J. Kant, *Tetrahedron: Asymmetry* **2002**, *13*, 349–355.
- [28] M. Kmetič, B. Stanovnik, *J. Heterocycl. Chem.* **1995**, *32*, 1563–1565.
- [29] L. Leite, M. Ramos, J. Bosco, M. P. Da Silva, A. Miranda, C. Fraga, E. Barreiro, *Farmacol.* **1999**, *54*, 747–757.
- [30] P. S. Branco, S. Prabhakar, A. M. Lobo, D. J. Williams, *Tetrahedron* **1992**, *48*, 6335–6360.
- [31] R. Urbanek, D. Brown, G. Steelman, W. Blackwell, S. Wesolowski, X. Wang (AstraZeneca), Int. Pat. WO/2007078251 (A1), **2007**.
- [32] D. Leung, W. Du, C. Hardouin, H. Cheng, I. Hwang, B. F. Cravatt, D. L. Boger, *Bioorg. Med. Chem. Lett.* **2005**, *15*, 1423–1428.
- [33] R. Huisgen, J. Sauer, H. J. Sturm, J. H. Markgraf, *Chem. Ber.* **1960**, *93*, 2106–2124.
- [34] K. Choi, A. D. Hamilton, *J. Am. Chem. Soc.* **2003**, *125*, 10241–10249.
- [35] K. Yang, B. Lou, *Mini-Rev. Med. Chem.* **2003**, *3*, 349–360.
- [36] Q. Huang, J. Mao, B. Wan, Y. Wang, R. Brun, S. G. Franzblau, A. P. Kozikowski, *J. Med. Chem.* **2009**, *52*, 6757–6767.
- [37] W. T. Lowther, B. W. Matthews, *Chem. Rev.* **2002**, *102*, 4581–4607.
- [38] S.-X. Xie, W.-J. Huang, Z.-Q. Ma, M. Huang, R. P. Hanzlik, Q.-Z. Ye, *Acta Crystallogr.* **2006**, *D62*, 425–432.
- [39] D. S. Kalinowski, D. R. Richardson, *Pharmacol. Rev.* **2005**, *57*, 547–583.
- [40] A. J. Copik, S. J. Swierczek, W. T. Lowther, V. M. D'souza, B. W. Matthews, R. C. Holz, *Biochemistry* **2003**, *42*, 6283–6292.
- [41] S. J. Watterson, S. Mitra, S. I. Swierczek, B. Bennett, R. C. Holz, *Biochemistry* **2008**, *47*, 11885–11893.
- [42] L. Mamelli, S. Petit, J. Chevalier, C. Giglione, A. Lieutaud, T. Meinnel, I. Artaud, J.-M. Pagès, *PLoS ONE* **2009**, *4*, e6443.
- [43] W.-L. Wang, S. C. Chai, M. Huang, H.-Z. He, T. D. Hurley, Q.-Z. Ye, *J. Med. Chem.* **2008**, *51*, 6110–6120.
- [44] H. Nikaido, *Microbiol. Mol. Biol. Rev.* **2003**, *67*, 593–656.
- [45] W. T. Lowther, D. A. McMillen, A. M. Orville, B. W. Matthews, *Proc. Natl. Acad. Sci. USA* **1998**, *95*, 12153–12157.
- [46] F. Frotin, A. Martinez, P. Peynot, S. Mitra, R. C. Holz, C. Giglione, T. Meinnel, *Mol. Cell. Proteomics* **2006**, *5*, 2336–2349.
- [47] S. Mitra, A. M. Dygas-Holz, J. Jiracek, M. Zertova, L. Zakova, R. C. Holz, *Anal. Biochem.* **2006**, *357*, 43–49.
- [48] A. G. W. Leslie, *Newsletter Prot. Crystallogr.* **1992**, *26*, 27–33.
- [49] P. Evans, *Acta Crystallogr. D* **2006**, *62*, 72–82.
- [50] Collaborative Computational Project Number 4, *Acta Crystallogr. D Biol. Crystallogr.* **1994**, *50*, 760–766.
- [51] W. T. Lowther, A. M. Orville, D. T. Madden, S. Lim, D. H. Rich, B. W. Matthews, *Biochemistry* **1999**, *38*, 7678–7688.
- [52] W. L. DeLano, The PyMOL Molecular Graphics System, **2002**, <http://www.pymol.org> (accessed March 15, 2012).

Received: February 6, 2012

Revised: March 7, 2012

Published online on ■■■■, 0000

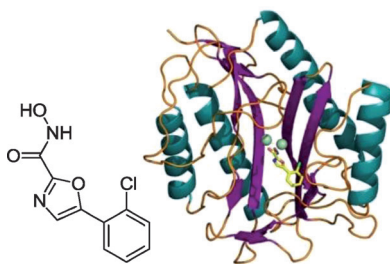
FULL PAPERS

F. Huguet, A. Melet, R. Alves de Sousa,
A. Lieutaud, J. Chevalier, L. Maigre,
P. Deschamps, A. Tomas, N. Leulliot,
J.-M. Pages, I. Artaud*

■■■ – ■■■



**Hydroxamic Acids as Potent Inhibitors
of Fe^{II} and Mn^{II} *E. coli* Methionine
Aminopeptidase: Biological Activities
and X-ray Structures of Oxazole
Hydroxamate–EcMetAP–Mn Complexes**



Great rings of five! New hydroxamic acids linked to furan, oxazole, oxadiazole, imidazole, and indole heterocycles were prepared and assayed against *E. coli* methionine aminopeptidase (EcMetAP). They showed selectivity for Mn^{II} and Fe^{II} metalloforms. Two X-ray crystal structures of oxazole hydroxamic acid–EcMetAP–Mn complexes were solved, and a molecular model of the indole derivative–EcMetAP–Mn complex was built.